Vanadium analogues of nonfunctionalized and amino-functionalized MOFs with MIL-101 topology: synthesis, characterization, and gas sorption properties

Shyam Biswas, Sarah Couck, Maciej Grzywa, Joeri F. M. Denayer, Dirk Volkmer, Pascal Van Der Voort

Angaben zur Veröffentlichung / Publication details:

Biswas, Shyam, Sarah Couck, Maciej Grzywa, Joeri F. M. Denayer, Dirk Volkmer, and Pascal Van Der Voort. 2012. "Vanadium analogues of nonfunctionalized and amino-functionalized MOFs with MIL-101 topology: synthesis, characterization, and gas sorption properties." European Journal of Inorganic Chemistry 2012 (15): 2481–86. https://doi.org/10.1002/ejic.201200106.

Vanadium Analogues of Nonfunctionalized and Amino-Functionalized MOFs with MIL-101 Topology – Synthesis, Characterization, and Gas Sorption Properties

Shyam Biswas,[a] Sarah Couck,[b] Maciej Grzywa,[c] Joeri F. M. Denayer,[b] Dirk Volkmer,[c] and Pascal Van Der Voort*[a]

Syntheses, characterization, and gas sorption properties of two new vanadium-based metal–organic frameworks $[V_3OCl(DMF)_2(BDC)_3]\cdot 3.1DMF\cdot 10H_2O\cdot 0.1BDC$ (V–MIL-101 or **1**) and $[V_3OCl(DMF)_2(BDC\text{–}NH_2)_3]\cdot 2.8DMF\cdot H_2O\cdot 0.1BDC\text{–}NH_2$ (V–MIL-101–NH_2 or **2**) (DMF = *N*,*N*′-dimethylformamide; BDC = terephthalate; BDC–NH_2 = 2-aminoterephthalate) having MIL-101 topology are presented. Compounds **1** and **2** were prepared under similar solvothermal conditions (150 °C, 24 h) in DMF by using VCl_3 and H_2BDC or $H_2BDC\text{–}NH_2$, respectively. Determination of lattice parameters from X-ray powder diffraction (XRPD) patterns of thermally activated compounds revealed their structural similarity with chromium-, iron-, and aluminum-based solids having two types of mesoporous cages and accessible metal sites. The phase purity of the compounds was ascertained by XRPD analysis, diffuse reflectance Fourier transform (DRIFT) spectroscopy, and elemental analysis. Thermogravimetric analyses (TGA) and temperature-dependent XRPD (TDXRPD) experiments indicate that the compounds are stable up to 320 and 240 °C, respectively, under an argon atmosphere. Removal of the guest DMF molecules by thermal activation enables the compounds to adsorb significant amounts of N_2 (690 and 555 $cm^3 g^{-1}$ at $p/p_0 = 1$ for **1** and **2**, respectively) and CO_2 (9.0 and 4.3 $mmol g^{-1}$ at 24.5 and 22.8 bar for **1** and **2**, respectively).

Introduction

Metal–organic frameworks (MOFs),[1–3] which are a class of highly crystalline and porous materials, have attracted a great deal of interest in recent years due to their wide range of potential applications in areas such as gas storage/separation,[4–6] catalysis,[7,8] and drug delivery.[9–12] The great success of this class of hybrid materials originated from the easy tunability of their structural topologies as well as their pore features (size, shape, chemical environment, etc.) by varying the type of metal source or organic linker (size, shape, or attached functional group) used during the synthesis. Among the various topological framework types known for MOFs, the MIL-*n* family of materials, originally developed by Férey's group, and a few other materials are of immense interest due to their high thermal and hydrolytic stability as well as enormous porosity.[13–16] For example, the chromium-based carboxylate MIL-101 (MIL: Materials of the Institute Lavoisier) with formula $[Cr_3F(H_2O)_2O(BDC)_3]\cdot nH_2O$ ($n \approx 25$) has a Langmuir surface area of 5900 $m^2 g^{-1}$ and contains two types of mesoporous cages having internal free diameters of approximately 29 and 34 Å.[13] Because of this unique feature, Cr–MIL-101 has been subject to a wide variety of applications such as catalysis,[17,18] gas sorption,[19–21] and controlled drug delivery.[9–12]

Inspired by the above-mentioned advantages and applications of Cr–MIL-101, we synthesized and fully characterized the vanadium analogue of nonfunctionalized and amino-functionalized MIL-101. It should be noted that nonfunctionalized as well as functionalized (with amino and nitro groups) MOFs with MIL-101 topology that incorporate chromium,[13,22,23] iron,[9,24] and aluminum[25] as metal atoms have formerly been reported. Our research group,[26] along with others,[27] has spent efforts in synthesizing vanadium-based MOFs because of their applicability in (selective) oxidation reactions. We have explored the remarkable heterogeneous catalytic performance of vanadium-based MIL-47 with low leaching in the oxidation of cyclohexene with *tert*-butyl hydroperoxide as oxidant.[28] Recently, our group has reported the synthesis and hetero-

[a] Department of Inorganic and Physical Chemistry,
Ghent University,
COMOC – Center for Ordered Materials, Organometallics and Catalysis,
Krijgslaan 281-S3, 9000 Ghent, Belgium
Fax: +32-92644983
E-mail: pascal.vandervoort@ugent.be
[b] Department of Chemical Engineering,
Vrije Universiteit
Brussel,
Pleinlaan 2, 1050 Brussel, Belgium
[c] Solid State and Materials Chemistry, Institute of Physics,
Augsburg University,
Universitaetsstrasse 1, 86159 Augsburg, Germany

geneous catalytic activity of a vanadium 2,6-naphthalenedicarboxylate, $[V^{IV}(OH)(O_2C–C_{10}H_6–CO_2)]$, denoted as COMOC-3 (COMOC: Center for Ordered Materials, Organometallics and Catalysis, Ghent University), in cyclohexene epoxidation.[29] In this article, we wish to report the synthesis, complete characterization, and gas sorption behavior of the two new vanadium-based MOFs $[V_3OCl(DMF)_2(BDC)_3]\cdot 3.1DMF\cdot 10H_2O\cdot 0.1BDC$ (V–MIL-101 or **1**) and $[V_3OCl(DMF)_2(BDC–NH_2)_3]\cdot 2.8DMF\cdot H_2O\cdot 0.1BDC–NH_2$ (V–MIL-101–NH_2 or **2**) (DMF = *N,N′*-dimethylformamide; BDC = terephthalate; BDC–NH_2 = 2-aminoterephthalate). Among the handful of porous vanadium-based MOFs (for example, MIL-47[30] and MIL-68[31]) documented in the literature, compound **1** possesses the second highest specific BET surface area, coming after the recently reported V–MIL-100 compound,[32] which also bears two types of mesoporous cages.

Results and Discussion

Starting from VCl_3 as metal source and BDC or BDC–NH_2 as organic linker, both V–MIL-101 and V–MIL-101–NH_2 can be synthesized in a wide variety of metal/linker molar ratios and temperatures (130–170 °C). The as-synthesized compounds were isolated with moderate crystallinity (Figures S1 and S2, Supporting Information). Their crystallinity increases significantly upon thermal activation (Figure 1 and Figure S3, Supporting Information).

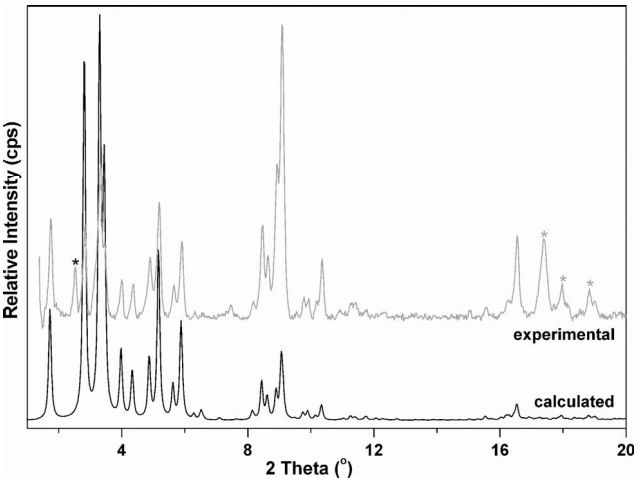

Figure 1. Calculated (black) XRPD pattern of Cr–MIL-101 and experimental (gray) XRPD pattern of activated **1** at room temperature recorded by protecting the air-sensitive sample with Kapton foil. Because activated **2** was less stable than activated **1** in air, a high-quality pattern of the former was impossible to collect with similar protection. The black and gray stars correspond to Bragg peaks due to the sample holder and an impure phase, respectively.

The diffuse reflectance infrared Fourier transform (DRIFT) spectra of isostructural **1** and **2** are similar, as expected. In the DRIFT spectra of as-synthesized **1** and **2** (Figures S4 and S5, Supporting Information), the strong absorption bands due to asymmetric and symmetric $–CO_2$ stretching vibrations of the coordinated terephthalate linker molecules are located at 1620 and 1440 cm^{-1}, respectively.[13] The characteristic strong absorption band of the carbonyl stretching vibration of the coordinated as well as guest DMF molecules appears at 1650 and 1660 cm^{-1} in the DRIFT spectra of as-synthesized **1** and **2**, respectively. The $–NH_2$ groups attached to coordinated BDC–NH_2 linker molecules give rise to medium absorption bands at 3301 and 3455 cm^{-1} in the DRIFT spectrum of as-synthesized **2**. The broad absorption band between 2500 and 3000 cm^{-1} observed in the DRIFT spectrum of as-synthesized **2** is due to the $–NH_2$ groups of free H_2BDC–NH_2 linker molecules encapsulated within the pores. The positions of the absorption bands of the $–NH_2$ groups are in agreement with those observed previously in Al–MIL-53–NH_2.[33]

Structure Description

The refined lattice parameters (Table 1) of thermally activated **1** determined from its room-temperature XRPD pattern (Figure 1) are similar to those of the known Cr–MIL-101 compound exhibiting a cubic structure. Compound **1** is thus isotypic with Cr–MIL-101, as also revealed by the similarity between their XRPD patterns (Figure 1). Since the structure of Cr–MIL-101 (Figure 2) is already reported,[13] a brief description of the framework structure of V–MIL-101 is presented here. The structure of V–MIL-101 (or V–MIL-101–NH_2) is built up of oxido-centered trimers $[V_3(\mu_3\text{-}O)Cl(DMF)_2]^{6+}$ that are composed of $[VO_6]$ octahedra. Notably, the existence of structurally similar trimeric units $[V_3(\mu_3\text{-}O)(H_2O)_3]^{7+}$ has been formerly observed in the vanadium 1,3-benzenedicaroboxylate denoted as MIL-59.[34] The trimers are interconnected by terephthalate linkers along the edges to form supertetrahedra (ST). The ST are further connected with each other in three-dimensional fashion to yield the augmented zeolite Mobil Thirty-Nine (MTN) type of framework. It is worth noting that the labile coordination sites of the $[VO_6]$ octahedra are occupied by O-donor atoms from DMF molecules or chlorine atoms, instead of fluorine atoms or water molecules as in the case of Cr–MIL-101. The existence of such coordinated DMF molecules in the MIL-101 structure has been verified by DRIFT spectroscopy and thermogravimetric and elemental analyses. The presence of coordinated chloride anions was confirmed by X-ray fluorescence (XRF) analysis. The framework is constructed from two types of mesoporous cages. The smaller cage is made up of 12 pentagonal rings with a free diameter of approximately 12 Å, and the diameter of the accessible cavity is approximately 29 Å. The larger cage includes 12 pentagonal and 4 hexagonal rings with a free diameter of the hexagonal rings of approxi-

Table 1. Refined lattice parameters for the M–MIL-101 (M^{3+} = V and Cr) solids having cubic unit cells.

Compound	*a* (Å)	*V* (Å^3)
V–MIL-101	88.77(3)	699548.8(48)
Cr–MIL-101[13]	88.869(1)	701860.3(1)

mately 14.5 by 16 Å and an accessible cage diameter of approximately 34 Å. The smaller and larger cages are present in a ratio of 2:1 consisting of 20 and 28 ST, respectively.

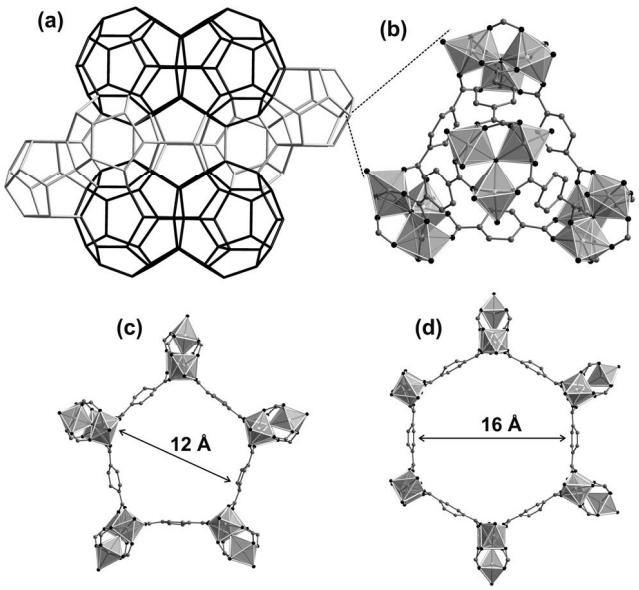

Figure 2. (a) MTN topological framework of Cr–MIL-101 having smaller (light gray) and larger (black) mesoporous cages. The structure is based on (b) supertetrahedra (ST), which consist of trimeric oxido-centered $[Cr_3(\mu_3\text{-}O)(F)(H_2O)_2]^{6+}$ units at the vertices interconnected by terephthalate linkers. The smaller and larger cages have only pentagonal (c) or a combination of pentagonal (c) and hexagonal (d) windows, respectively. Color codes: Cr, light gray octahedra; C, dark gray; O, black. The MTN framework (a) and the parts of Cr–MIL-101 (b–d) have been drawn by using the atomic coordinates provided in "Database of Zeolite Structures"[40] and ref.,[13] respectively.

It should be mentioned here that the assignment of the terminal ligands attached to the vanadium atoms of the oxido-centered trinuclear units is based on the fact that the chlorine atoms and DMF molecules present in a ratio of 1:2 render the structure electrostatically neutral. There are no anions present in the reaction medium, and the existence of hydroxide anions in the structure can be ruled out, as evidenced by the DRIFT spectra of the compounds (Figures S4 and S5). It was impossible to obtain single crystals of the compounds, hampering single-crystal X-ray analysis, which might strongly support the assignment of the terminal ligands. The quantitative assignment of the terminal ligands by spectroscopic methods (DRIFT, TG, XRF, and elemental analysis) is thus tentative, since some of the ligands (Cl and DMF) assigned to be located at terminal positions might also correspond to the guest species inside the pores. For example, a recent investigation of the Al–MIL-100 structure by solid-state NMR spectroscopy has shown that different species (nitrate, unreacted trimesate, and water) are also present within the cavities.[35] Notably, the coordination of chloride anions with the vanadium atoms has been formerly observed in V–MIL-100.[32] Moreover, DMF molecules have been found to coordinate with vanadium(III) ions in several complexes.[36]

TGA and XRPD

The phase purity of **1** and **2** were examined by using XRPD patterns recorded from as-synthesized **1** and **2** at ambient conditions. The experimental XRPD patterns of as-synthesized **1** and **2** (Figures S1 and S2, Supporting Information) are consistent with simulated patterns documented for pristine Cr–MIL-101. The compounds retain their crystallinity upon heating (130 °C, **1**; 100 °C, **2**) for 12 h under dynamic vacuum (i.e., activation), as verified by the XRPD patterns of the corresponding samples (Figure 1 and Figure S3, Supporting Information).

TGA and temperature-dependent XRPD (TDXRPD) experiments were performed to examine the thermal stability of both compounds. From the TG analyses, it is observed that as-synthesized **1** and **2** decompose above 320 and 240 °C, respectively, under a helium atmosphere. The lower thermal stability obtained from TG analyses (2 °C min^{-1}) relative to that determined by TDXRPD measurements (6 °C min^{-1}) is due to the slower heating rate used in the former measurement. It is worth noting that both compounds are sensitive to air and moisture, and decompose within a few hours in air.

In the TG curve of as-synthesized **1** (Figure 3a), the first weight loss of 46.2% in the range 70–200 °C is attributed to the removal of 5.1 DMF, 10 water, and 0.1 BDC molecules per formula unit (calcd. 46.3%). The second weight loss of 28.6% in the range 280–400 °C is due to the decomposition of the framework, which leads to the formation of crystalline V_2O_5.

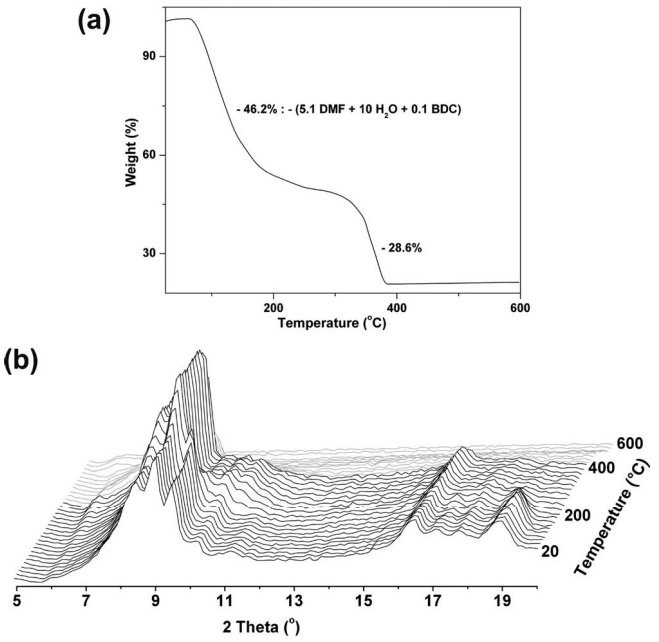

Figure 3. (a) TG analysis of as-synthesized **1** under argon. (b) TDXRPD patterns of as-synthesized **1** measured under a helium atmosphere in the range 20–600 °C. The black and gray patterns denote stable and decomposed phases, respectively.

TDXRPD analysis (Figure 3b and Figure S6, Supporting Information) shows that as-synthesized **1** is stable up to

400 °C. After that, the compound starts to decompose and becomes completely amorphous at 500 °C.

In the TG curve of as-synthesized **2** (Figure 4a), the first weight loss of 34.2% in the range 80–210 °C is assigned to the loss of 4.8 DMF, one water, and 0.1 BDC–NH_2 molecules per formula unit (calcd. 34.3%). The second weight loss of 43.4% in the range 210–400 °C is due to the decomposition of the material resulting in the formation of V_2O_5.

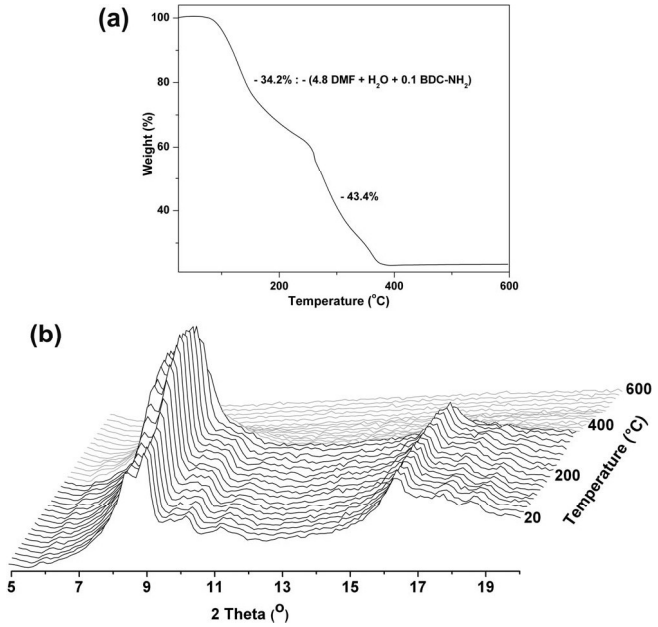

Figure 4. (a) TG analysis of as-synthesized **2** under argon. (b) TDXRPD patterns of as-synthesized **2** measured under a helium atmosphere in the range 20–600 °C. The black and gray patterns denote stable and decomposed phases, respectively.

From the TDXRPD patterns (Figure 4b and Figure S7, Supporting Information), it becomes obvious that as-synthesized **2** is stable up to 340 °C. After that, the material starts to decompose and becomes completely amorphous at 400 °C.

Gas Sorption Properties

N_2 and CO_2 sorption isotherms were determined on thermally activated **1** and **2**. The results of the sorption analyses are presented in Table 2. The N_2 sorption capacities of the present compounds are comparable with those of the previously reported Al–MIL-101–NH_2,[25] Cr–MIL-101–NO_2,[23] and Cr–MIL-101–NH_2,[23] but they are significantly lower than those of Cr–MIL-101,[13] Fe–MIL-101,[9] and Fe–MIL-101–NH_2.[37] The considerably lower specific BET surface area of **1** compared to that of its chromium analogue can be ascribed to the occurrence of a secondary phase (Figure 1) during the synthesis as well as the difficulty of removing the guest DMF molecules from the pores due to the lower thermal stability of the compound. It is noteworthy that V–MIL-101 (2118 $m^2 g^{-1}$) possesses the second highest specific BET surface area among the vanadium-containing MOFs reported in the literature, after the recently reported V–MIL-100[32] (2320 $m^2 g^{-1}$).

Table 2. Results of sorption analysis for the M–MIL-101–X (M^{3+} = Cr, Fe, Al; X = H, NO_2, NH_2) solids.

Compound	BET surface area[a] ($m^2 g^{-1}$)	Langmuir surface area[a] ($m^2 g^{-1}$)	CO_2 uptake[c] (mmol g^{-1})
V–MIL-101	2118	3032	9.0 (24.5, 300)
V–MIL-101–NH_2	1623	–	4.3 (22.8, 300)
Cr–MIL-101[13,19]	4100	5900	20 (30.0, 303)
Cr–MIL-101–NO_2[23]	1425	–	–
Cr–MIL-101–NH_2[23]	2313	–	–
Fe–MIL-101[9]	–	4535	–
Fe–MIL-101–NH_2[41]	–[b]	–	–
Al–MIL-101–NH_2[25]	2100	–	14 (30.0, 298)

[a] The specific surface areas have been calculated from the N_2 adsorption isotherms. [b] The adsorption capacity at p/p_0 = 1 is 1100 $cm^3 g^{-1}$. [c] The first and the second values within parentheses represent the pressure (bar) and the temperature (K), respectively, at which the uptake is achieved.

The N_2 adsorption and desorption measurements carried out with thermally activated **1** and **2** revealed reversible type-I isotherms (Figure 5) with a small step in the adsorption curve at p/p_0 = 0.2. The shapes of the isotherms are similar to the those of the isostructural M–MIL-101–X compounds reported in the literature.[9,13,23,25,41]

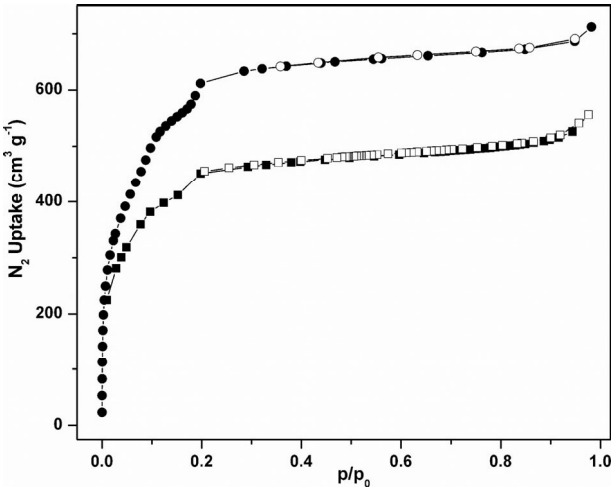

Figure 5. Low-pressure N_2 adsorption (solid symbols) and desorption (empty symbols) isotherms of thermally activated **1** (circles) and **2** (squares) measured at –196 °C.

As shown in Figure 6, the CO_2 adsorption isotherms of thermally activated **1** and **2** follow type-I behavior in the pressure range from 0 to 25 bar at 27 °C. The CO_2 uptake of **1** (Table 2) is slightly lower than that of Al–MIL-101–NH_2 reported formerly,[25] but it is significantly lower than that of Cr–MIL-101.[19] This CO_2 uptake trend is in agreement with the specific surface area of the compounds. The surprisingly lower CO_2 uptake of **2** compared to those of the other isostructural compounds can be attributed to the

difficulty of removing the occluded DMF molecules from the pores due to the lower thermal stability of the compound, which results in a considerable decrease in the accessible surface area. The blocking of the entrance by the attached $-NH_2$ groups positioned in the cage windows is another reason for the lower CO_2 uptake of **2**.

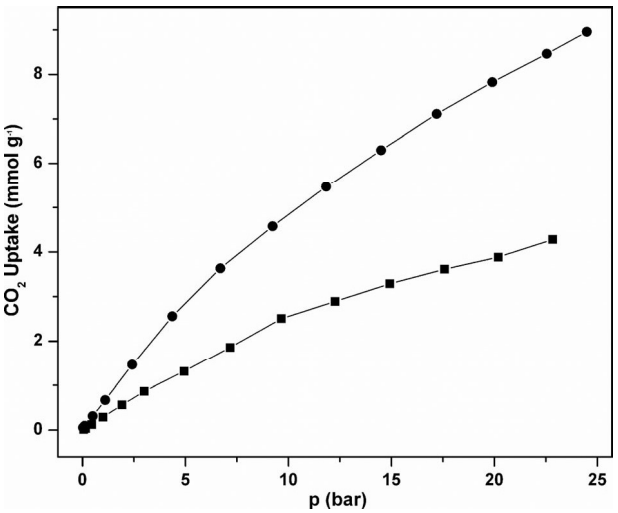

Figure 6. High-pressure CO_2 adsorption isotherms of thermally activated **1** (circles) and **2** (squares) measured at 27 °C.

Conclusions

We have successfully prepared and thoroughly characterized two redox-active, vanadium-based MOFs, V–MIL-101 (**1**) and V–MIL-101–NH_2 (**2**), having accessible vanadium sites. The phase purity of the compounds was confirmed by a combination of XRPD analysis, DRIFT spectroscopy, and elemental analysis. TGA and temperature-dependent XRPD experiments show that the compounds possess moderate thermal stability (320 °C, **1**; 240 °C, **2**) under argon. N_2 and CO_2 sorption measurements reveal significantly high uptakes, which suggest that the compounds are potential candidates for gas storage applications, provided that the samples are handled under an inert atmosphere. Finally, the redox activity of vanadium(III) atoms paired with the availability of coordinatively unsaturated vanadium sites would make the compounds useful in heterogeneous catalytic reactions, in which the presence of air and moisture must be avoided.

Experimental Section

Materials and General Methods: All starting materials were of reagent grade and used as received from the commercial supplier. VCl_3 was weighed in a nitrogen-filled glove box. The thermally activated samples were also stored in a glove box because of their air-sensitivity. All other manipulations were carried out under an air atmosphere. Diffuse-reflectance infrared Fourier transform (DRIFT) spectra were recorded with a Thermo Nicolet 6700 FTIR spectrometer equipped with a nitrogen-cooled MCT detector and a KBr beam splitter. The DRIFT cell was connected to a vacuum manifold. The following indications are used to characterize absorption bands: very strong (vs), strong (s), medium (m), weak (w), shoulder (sh), and broad (br). Elemental analyses (C, H, N) were carried out with a Thermo Scientific Flash 2000 CHNS-O analyzer equipped with a TCD detector. Thermogravimetric analysis (TGA) was performed with a Netzsch STA-409CD thermal analyzer in a temperature range of 25–600 °C under an argon atmosphere at a heating rate of 2 °C min^{-1}. Ambient temperature X-ray powder diffraction (XRPD) patterns were recorded with a Seifert XRD 3003 TT diffractometer outfitted with a Meteor 1D detector and automatic divergence slits (for activated **1**) or a Thermo Scientific ARL X'Tra diffractometer (for all other compounds), both operated at 40 kV, 40 mA with Cu-K_α (λ = 1.5406 Å) radiation. Lattice parameters were determined by using the DICVOL program[38] and refined with the STOE's WinXPow[39] software package. Temperature-dependent XRPD patterns were collected with a Bruker D8 Discover X-ray diffractometer with a linear detector; the XRD patterns were recorded from room temperature to 600 °C with a temperature ramp of 0.1 °C s^{-1} in helium flow. The nitrogen sorption isotherms up to 1 bar were measured by using a Belsorp Mini apparatus at –196 °C. The high-pressure carbon dioxide sorption isotherms were recorded with a volumetric HPA 100 from VTI at 27 °C. The samples were heated (130 °C, **1**; 100 °C, **2**) under dynamic vacuum for 12 h prior to the sorption experiments.

Syntheses

$[V_3OCl(C_3H_7NO)_2(C_8H_4O_4)_3]\cdot 3.1C_3H_7NO\cdot 10H_2O\cdot 0.1C_8H_6O_4$ (1): A mixture of VCl_3 (200 mg, 1.27 mmol) and terephthalic acid (106 mg, 0.64 mmol) in DMF (2 mL) was placed in a Pyrex tube (10 mL). The tube was sealed and heated in a preheated heating block to 150 °C, held at this temperature for 24 h, then cooled spontaneously to room temperature. The green precipitate was collected by filtration, washed with DMF (2 ×3 mL), and dried in air to yield **1** (160 mg, 0.10 mmol, 31%). $C_{40.1}H_{68.1}ClN_{5.1}O_{28.5}V_3$ (1265.96): calcd. C 38.04, H 5.42, N 5.64; found C 38.30, H 5.32, N 5.66. DRIFT (KBr): 2928 (br), 2440 (m), 1715 (w), 1651 (s), 1619 (sh), 1512 (m), 1430 (sh), 1404 (vs), 1302 (w), 1256 (m), 1158 (w), 1103 (m), 1062 (w), 1021 (m), 990 (m), 939 (w), 883 (w), 827 (w), 806 (w), 778 (w), 743 (s), 697 (m), 666 (w) cm^{-1}.

$[V_3OCl(C_3H_7NO)_2(C_8H_5NO_4)_3]\cdot 2.8C_3H_7NO\cdot H_2O\cdot 0.1C_8H_7NO_4$ (2): A mixture of VCl_3 (200 mg, 1.27 mmol) and 2-aminoterephthalic acid (116 mg, 0.64 mmol) in DMF (2 mL) was placed in a Pyrex tube (10 mL). The tube was sealed and heated in a preheated heating block to 150 °C, held at this temperature for 24 h, then cooled spontaneously to room temperature. The green precipitate was collected by filtration, washed with DMF (2× 3 mL), and dried in air to yield **2** (130 mg, 0.12 mmol, 29%). $C_{39.2}H_{51.1}ClN_{7.9}O_{19.2}V_3$ (1128.44): calcd. C 41.72, H 4.56, N 9.80; found C 41.74, H 4.72, N 9.85. DRIFT (KBr): 3454 (m), 3301 (br), 2934 (br), 2768 (br), 2438 (m), 1658 (s), 1617 (sh), 1499 (m), 1438 (sh), 1387 (s), 1341 (w), 1260 (s), 1162 (w), 1098 (m), 1060 (w), 1025 (w), 974 (m), 891 (w), 836 (w), 800 (w), 764 (s), 698 (w), 660 (w) cm^{-1}.

Supporting Information (see footnote on the first page of this article): XRPD patterns and DRIFT spectra.

Acknowledgments

The authors would like to thank Department of Solid State Sciences, Ghent University, for temperature-dependent XRPD measurements. This research is funded by Ghent University, GOA grant number 01G00710.

[1] G. Férey, *Chem. Soc. Rev.* **2008**, *37*, 191–214.

[2] S. Kitagawa, R. Kitaura, S. Noro, *Angew. Chem.* **2004**, *116*, 2388–2430; *Angew. Chem. Int. Ed.* **2004**, *43*, 2334–2375.

[3] O. M. Yaghi, M. O'Keeffe, N. W. Ockwig, H. K. Chae, M. Eddaoudi, J. Kim, *Nature* **2003**, *423*, 705–714.

[4] L. J. Murray, M. Dincă, J. R. Long, *Chem. Soc. Rev.* **2009**, *38*, 1294–1314.

[5] J.-R. Li, R. J. Kuppler, H.-C. Zhou, *Chem. Soc. Rev.* **2009**, *38*, 1477–1504.

[6] L. Hamon, P. L. Llewellyn, T. Devic, A. Ghoufi, G. Clet, V. Guillerm, G. D. Pirngruber, G. Maurin, C. Serre, G. Driver, W. van Beek, E. Jolimaitre, A. Vimont, M. Daturi, G. Férey, *J. Am. Chem. Soc.* **2009**, *131*, 17490–17499.

[7] J. Lee, O. K. Farha, J. Roberts, K. A. Scheidt, S. T. Nguyen, J. T. Hupp, *Chem. Soc. Rev.* **2009**, *38*, 1450–1459.

[8] L. Ma, C. Abney, W. Lin, *Chem. Soc. Rev.* **2009**, *38*, 1248–1256.

[9] K. M. L. Taylor-Pashow, J. Della Rocca, Z. G. Xie, S. Tran, W. B. Lin, *J. Am. Chem. Soc.* **2009**, *131*, 14261–14263.

[10] P. Horcajada, T. Chalati, C. Serre, B. Gillet, C. Sebrie, T. Baati, J. F. Eubank, D. Heurtaux, P. Clayette, C. Kreuz, J. S. Chang, Y. K. Hwang, V. Marsaud, Y.-N. Bories, L. Cynober, S. Gil, G. Férey, P. Couvreur, R. Gref, *Nat. Mater.* **2010**, *9*, 172–178.

[11] M. Vallet-Regí, F. Balas, D. Arcos, *Angew. Chem.* **2007**, *119*, 7692–7703; *Angew. Chem. Int. Ed.* **2007**, *46*, 7548–7558.

[12] P. Horcajada, C. Serre, M. Vallet-Regí, M. Sebban, F. Taulelle, G. Férey, *Angew. Chem.* **2006**, *118*, 6120–6124; *Angew. Chem. Int. Ed.* **2006**, *45*, 5974–5978.

[13] G. Férey, C. Mellot-Draznieks, C. Serre, F. Millange, J. Dutour, S. Surble, I. Margiolaki, *Science* **2005**, *309*, 2040–2042.

[14] J. H. Cavka, S. Jakobsen, U. Olsbye, N. Guillou, C. Lamberti, S. Bordiga, K. P. Lillerud, *J. Am. Chem. Soc.* **2008**, *130*, 13850–13851.

[15] C. Serre, F. Millange, C. Thouvenot, M. Noguès, G. Marsolier, D. Louër, G. Férey, *J. Am. Chem. Soc.* **2002**, *124*, 13519–13626.

[16] M. Dan-Hardi, C. Serre, T. Frot, L. Rozes, G. Maurin, C. Sanchez, G. Férey, *J. Am. Chem. Soc.* **2009**, *131*, 10857–10859.

[17] A. Henschel, K. Gedrich, R. Kraehnert, S. Kaskel, *Chem. Commun.* **2008**, 4192–4194.

[18] N. V. Maksimchuk, M. N. Timofeeva, M. S. Melgunov, A. N. Shmakov, Y. A. Chesalova, D. N. Dybtsev, V. P. Fedin, O. A. Kholdeeva, *J. Catal.* **2008**, *257*, 315–323.

[19] P. L. Llewellyn, S. Bourrelly, C. Serre, A. Vimont, M. Daturi, L. Hamon, G. DeWeireld, J.-S. Chang, D.-Y. Hong, Y. K. Hwang, S. H. Jhung, G. Férey, *Langmuir* **2008**, *24*, 7245–7250.

[20] S. H. Jhung, J.-H. Lee, J. W. Yoon, C. Serre, G. Férey, J.-S. Chang, *Adv. Mater.* **2007**, *19*, 121–124.

[21] M. Latroche, S. Surble, C. Serre, C. Mellot-Draznieks, P. L. Llewellyn, J.-H. Lee, J.-S. Chang, S. H. Jhung, G. Férey, *Angew. Chem.* **2006**, *118*, 8407–8411; *Angew. Chem. Int. Ed.* **2006**, *45*, 8227–8231.

[22] A. Sonnauer, F. Hoffmann, M. Fröba, L. Kienle, V. Duppel, M. Thommes, C. Serre, G. Férey, N. Stock, *Angew. Chem.* **2009**, *121*, 3849–3852; *Angew. Chem. Int. Ed.* **2009**, *48*, 3791–3794.

[23] S. Bernt, V. Guillerm, C. Serre, N. Stock, *Chem. Commun.* **2011**, *47*, 2838–2840.

[24] S. Bauer, C. Serre, T. Devic, P. Horcajada, J. Marrot, G. Férey, N. Stock, *Inorg. Chem.* **2008**, *47*, 7568–7576.

[25] P. Serra-Crespo, E. V. Ramos-Fernandez, J. Gascon, F. Kapteijn, *Chem. Mater.* **2011**, *23*, 2565–2572.

[26] K. Leus, I. Muylaert, M. Vandichel, G. B. Marin, M. Waroquier, V. Van Speybroeck, P. Van der Voort, *Chem. Commun.* **2010**, *46*, 5085–5087.

[27] A. Phan, A. U. Czaja, F. Gándara, C. B. Knobler, O. M. Yaghi, *Inorg. Chem.* **2011**, *50*, 7388–7390.

[28] K. Leus, M. Vandichel, Y.-Y. Liu, I. Muylaert, J. Musschoot, S. Pyl, H. Vrielinck, F. Callens, G. B. Marin, C. Detavernier, P. V. Wiper, Y. Z. Khimyak, M. Waroquier, V. Van Speybroeck, P. Van Der Voort, *J. Catal.* **2012**, *285*, 196–207.

[29] Y.-Y. Liu, K. Leus, M. Grzywa, D. Weinberger, K. Strubbe, H. Vrielinck, R. Van Deun, D. Volkmer, V. Van Speybroeck, P. Van Der Voort, *Eur. J. Inorg. Chem.* **2011**, DOI: 10.1002/ejic.201101099.

[30] K. Barthelet, J. Marrot, D. Riou, G. Férey, *Angew. Chem.* **2002**, *114*, 291; *Angew. Chem. Int. Ed.* **2002**, *41*, 281–284.

[31] K. Barthelet, J. Marrot, G. Férey, D. Riou, *Chem. Commun.* **2004**, 520–521.

[32] A. Lieb, H. Leclerc, T. Devic, C. Serre, I. Margiolaki, F. Mahjoubi, J. S. Lee, A. Vimont, M. Daturi, J.-S. Chang, *Microporous Mesoporous Mater.* **2011**, DOI: 10.1016/j.micromeso.2011.12.001.

[33] T. Ahnfeldt, D. Gunzelmann, T. Loiseau, D. Hirsemann, J. Senker, G. Férey, N. Stock, *Inorg. Chem.* **2009**, *48*, 3057–3064.

[34] K. Barthelet, D. Riou, G. Férey, *Chem. Commun.* **2002**, 1492–1493.

[35] M. Haouas, C. Volkringer, T. Loiseau, G. Férey, F. Taulelle, *J. Phys. Chem. C* **2011**, *115*, 17934–17944.

[36] a) C. C. McLauchlan, K. J. McDonald, *Acta Crystallogr., Sect. E Struct. Rep. Online* **2006**, *62*, m588–m590; b) M. P. Weberski Jr., C. C. McLauchlan, *Inorg. Chem. Commun.* **2007**, *10*, 906–909; c) C. J. Carrano, M. Mohan, S. M. Holmes, R. de la Rosa, A. Butler, J. M. Charnock, C. D. Garner, *Inorg. Chem.* **1994**, *33*, 646–655; d) N. S. Dean, L. M. Mokry, M. R. Bond, C. J. O'Connor, C. J. Carrano, *Inorg. Chem.* **1996**, *35*, 2818–2825.

[37] C. Scherb, J. J. Williams, F. Hinterholzinger, S. Bauer, N. Stock, T. Bein, *J. Mater. Chem.* **2011**, *21*, 14849–14856.

[38] A. Boultif, D. J. Louer, *Appl. Crystallogr.* **1991**, *24*, 987–993.

[39] *STOE WinXPOW* version 2.11, Stoe & Cie GmbH, Darmstadt, Germany, **2005**.

[40] http://www.iza-structure.org/databases/.

[41] C. Scherb, J. J. Williams, F. Hinterholzinger, S. Bauer, N. Stock, T. Bein, *J. Mater. Chem.* **2011**, *21*, 14849–14856.